

## Probes of the solar interior

S.M. Chitre and H.M. Antia

*Tata Institute of Fundamental Research, Homi Bhabha Road, Mumbai 400 005, India*

**Abstract.** The interior of the Sun is not directly accessible to observations. Nonetheless, it is possible to infer the physical conditions prevailing in the solar interior with the help of theory of stellar structure and the powerful observational input provided by the measurements of solar neutrino fluxes and by the accurate helioseismic data. It turns out that the standard solar model gives a satisfactory description of the thermal profile throughout the Sun's inside. A cooler solar core is therefore, not a viable solution to account for the deficit in the measured solar neutrino fluxes, and the answer to the solar neutrino puzzle should probably be sought in the realm of particle physics.

*Key words:* sun: oscillations, sun: interior

### 1. Introduction

Even though the inside of our Sun is not directly accessible to observations, it is nevertheless, possible to infer its internal structure. This can be achieved using the set of mathematical equations describing the mechanical and thermal equilibrium for a spherical star together with the boundary conditions. The conventional approach is to assume the Sun to have a homogeneous initial chemical composition and the mass ( $M_{\odot}=1.989\times 10^{33}$  gm) and then to evolve it to have the present luminosity ( $L_{\odot}=3.846\times 10^{33}$  erg s<sup>-1</sup>) and radius ( $R_{\odot}=6.960\times 10^{10}$  cm) after 4.6 billion years (its estimated age), with a couple of adjustable parameters. Our knowledge of the Sun's interior is mainly based on extensive numerical computations. The central question has been whether there is any way of checking the correctness of these theoretical models describing the internal structure of the Sun.

### 2. Standard solar model and the structure equations

The so-called standard solar model is based on the following set of simplifying assumptions:

- (i) The Sun is spherically symmetric with negligible effects of rotation, magnetic field and mass loss on its structure.

- (ii) The Sun is in mechanical and thermal equilibrium, with uniform initial chemical composition.
- (iii) The energy is generated in the inner core by thermonuclear burning of hydrogen into helium and it is transported by radiative processes through the layers of the Sun which are stable against convection.
- (iv) The standard physics like equation of state, opacities, nuclear reaction rates and properties of neutrinos is applicable while constructing solar models.

The equations governing hydrostatic and thermal equilibrium may be expressed as follows:

$$\text{Mechanical : } \frac{dP(r)}{dr} = \frac{-Gm(r)}{r^2} \rho(r), \quad \frac{dm(r)}{dr} = 4\pi r^2 \rho(r), \quad (1)$$

where  $P(r)$  is the pressure,  $\rho(r)$ , the density and  $m(r)$ , the mass interior to radius  $r$  for a spherical star.

$$\text{Thermal : } \frac{dL(r)}{dr} = 4\pi r^2 \rho(r) \epsilon, \quad (2)$$

where  $L(r)$  is the luminosity and  $\epsilon$ , the nuclear energy generation rate per unit mass. The thermonuclear energy production is largely (~99%) contributed by the proton-proton chain (Bahcall 1989).

The energy generated in the central regions of the Sun is transported to the surface, from where it escapes into the space outside, mainly by radiative processes through much of the solar interior. This radiative flux,  $F_{\text{rad}}$  is related to the temperature gradient by the equation of radiative transfer,

$$F_{\text{rad}} = \frac{16\sigma T^3}{3\kappa\rho} \frac{dT}{dr}, \quad (3)$$

where  $\sigma$  is the Stefan-Boltzmann constant and  $\kappa$  the opacity of the solar material. In the region where hydrogen and helium are undergoing ionization ( $T \approx 10^4$  K) the opacity rises very sharply, thus increasing the temperature gradient,  $\nabla = \frac{d \ln T}{d \ln P}$ , while the corresponding adiabatic gradient,  $\nabla_{\text{ad}} = \left(\frac{d \ln T}{d \ln P}\right)_{\text{ad}}$  is diminished to satisfy the criterion of superadiabaticity for the onset of convection. In the region unstable to convection, the convective flux,  $F_{\text{conv}}$  is then constructed adopting a mixing-length prescription (Cox & Giuli 1968).

The foregoing structure equations need to be supplemented by auxiliary equations which incorporate the input physics describing the thermodynamic state of matter through the equation of state (cf., Rogers et al. 1996), the Rosseland mean opacity of solar material  $\kappa = \kappa(\rho, T, X, Y, Z)$  (cf., Rogers & Iglesias 1992) and the nuclear energy generation rate,  $\epsilon = \epsilon(\rho, T, X, Y, Z)$  (cf., Bahcall 1989). Here,  $X, Y, Z$  are respectively the hydrogen, helium and heavy element abundances by mass. Another effect which has been included in the standard solar model is the diffusion of helium and heavy elements relative to hydrogen, leading to a change in the composition profile in the radiative interior. The diffusive process could arise from the effects due mainly to gravitational settling because of momentum-exchange between heavier and lighter elements and also to some extent on account of thermal gradients (Guzik & Cox 1993). The solar model is constructed by numerical integration of the structure

equations together with the auxiliary equations and appropriate boundary conditions. The outstanding problem of solar physics has been whether there is any way of "seeing" into the interior of the Sun and testing how far the theoretical models are tenable.

### 3. Probes of the solar interior

For over three decades, there have been attempts to measure the flux of neutrinos generated by the reaction network operating in the solar core. Davis' chlorine experiment which was the first diagnostic probe designed to infer the physical conditions inside the Sun, reports the measured solar neutrino flux to be  $2.55 \pm 0.25$  SNU (1 SNU =  $10^{-36}$  captures per target atom per second). The predicted capture rate for the chlorine experiment calculated by Bahcall & Pinsonneault (1995) for a standard solar model with improved opacities and equation of state is  $9.5^{+1.2}_{-1.4}$  SNU. There is clearly a deficit, by over a factor of 3 of the measured neutrino flux over the predicted flux from a standard solar model. The two other radiochemical experiments which use the gallium detector are sensitive to the lower energy neutrinos. The measured solar neutrino counting rate is  $74 \pm 8$  SNU, while the theoretically predicted neutrino capture rate for the gallium experiment is  $137^{+8}_{-7}$  SNU. The measured flux is thus nearly half of that predicted by a standard solar model. The Kamiokande experiment in an underground mine uses a water detector for capturing high energy neutrinos. Again the measured rate of neutrino events recorded by Kamiokande setup is deficient by about 50% of the theoretically predicted values.

We thus have a clear discrepancy between measured and predicted neutrino fluxes if we assume the neutrinos to have standard physical properties, namely, no mass, no magnetic moment, no flavour-mixing. There have been, over the years, a number of ingenious suggestions to account for the observed deficit of solar neutrino flux by resorting to a non-standard solar model. These include the presence of a centrally concentrated magnetic field, the rapidly rotating core, lower heavy element abundance (and hence reduced opacities), partial mixing in the central region which brings additional fuel of hydrogen into the energy-generating core, the presence of weakly interacting massive particles in the core which effectively increases its thermal conductivity. Admittedly, all these solutions can cause a lowering of the neutrino flux, but they lead to a larger suppression of the high-energy neutrinos to which Kamiokande detector is sensitive and there appears to be an anomaly in the measurement of relative neutrino fluxes from different experiments. A possible resolution of this paradox is MSW effect (cf., Pal 1997) which is based on the electron neutrinos, generated in the solar core and endowed with a tiny mass, getting transformed during the transit through the solar body, into neutrinos of a different flavour which thus go undetected in the current neutrino experiments.

Such a paradoxical situation has prompted solar physicists to look for some independent means to determine conditions in the interior of the Sun. Since the early 1960s it has been noticed that the solar surface undergoes a series of mechanical vibrations. These manifest as Doppler shifts oscillating through a cycle with a period around five minutes (Leighton et al. 1962). Such a tool provided by the rich spectrum of velocity fields observed at the solar surface whose frequencies are determined with great accuracy (better than 1 part in  $10^5$ ), probes the Sun's interior with extraordinary precision. Solar oscillations may be regarded as a superposition of many standing waves which sample many different layers of the Sun and their frequencies depend on the average internal properties like the density, temperature and

chemical composition of the solar material. In much the same manner as the study of seismic waves generated by earthquakes has helped us to learn about the interior of the earth, it was hoped that helioseismology will enable us to infer the physical conditions like the density and sound speed inside the Sun. It turns out that the accurately determined seismic data has a stronghold on permissible solar models.

The rich spectrum of over ten million acoustic modes generated by the oscillating Sun has yielded valuable information about the solar interior. The helioseismic data has been analysed in two ways: (i) Direct model fitting; (ii) Inversion methods. In the direct or forward method, the equations of stellar structure are used to construct a set of models with different values of one or more adjustable parameters. The equilibrium models are perturbed to obtain the linear eigenfrequencies of solar oscillations which could then be compared with the accurately measured *p*-mode frequencies. In practice, the fit cannot, of course, be perfect, but there are indications that the depth of the solar convection zone is  $\approx 200,000$  km, which is deeper than what was previously estimated, and the helium abundance by mass in the solar envelope is  $\approx 0.25$ . An analysis of the oscillation frequencies also suggested that the computed opacities near the base of the convection zone were too low, a result which was later confirmed by the more up-to-date Livermore opacity calculations (Rogers & Iglesias 1992).

The forward method has had only a limited success and more recently, the inversion techniques have been effectively adopted to extract the physical conditions in the solar interior from the accurate information available on the *p*-modes. One of the major accomplishments of the inversion method is that the sound speed is now known through the bulk of the solar interior to an accuracy of better than 0.1% and the density and pressure are known to somewhat lower accuracy (Gough et al. 1996). Fig. 1 displays the model profiles for the density,  $\rho$  and sound speed,  $c_s = (\Gamma_1 P / \rho)^{1/2}$ , where  $\Gamma_1 = (\frac{\partial \ln P}{\partial \ln \rho})_s$  is the adiabatic index. The solar models have been refined over the years with better input physics as is clear from this figure. With the help of the sound speed and density inferred from the helioseismic data, it is possible to determine the variation of the adiabatic index  $\Gamma_1$  in the ionization zones which enables one to obtain the helium abundance in the solar envelope (Basu & Antia 1995).

The depth of the convection zone is inferred to be  $0.287R_\odot$  from an analysis of the function,  $W(r) = (1/g) \frac{dc^2}{dr}$  showing a sharp rise at the base of the convection zone introduced by an abrupt transition in the temperature gradient from the adiabatic to the radiative value (Christensen-Dalsgaard et al. 1991). Likewise, the convective overshoot below the convection zone may be surmised by analysing the characteristic oscillatory component introduced in the *p*-mode frequencies by the discontinuity in the derivatives of the sound speed. The extent of the convective overshoot is estimated to be less than  $0.1H_p$  (Basu et al. 1994; Monteiro et al. 1994).

The seismic inversions which have provided the foregoing information about the solar interior are based only on the mechanical constraints (Eq. 1). In order to infer the thermal and chemical composition profiles through the solar body, one needs to invoke the equations of thermal balance and energy transport (Eq. 2,3) together with the auxiliary input provided by the opacity, nuclear energy generation rate and equation of state (cf., Antia and Chitre 1995; Shibahashi & Takata 1996; Kosovichev). Once the temperature, density and composition

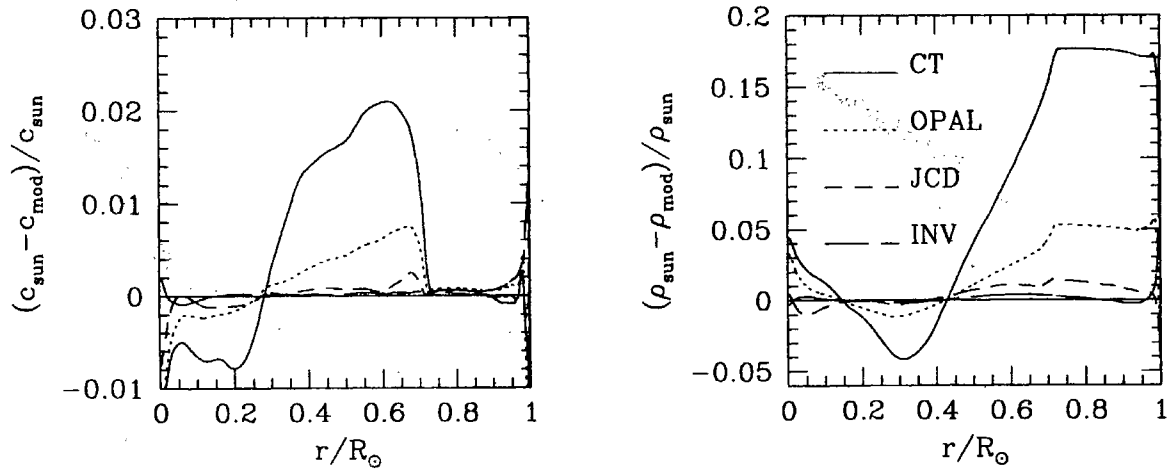


**Figure 1.** Relative difference in sound speed and density between some solar models and the Sun as inferred from helioseismic inversion. Model CT has been constructed using the opacity tables of Cox and Tabor (1976) and does not incorporate any diffusion, Model OPAL uses the more recent OPAL opacities, Model JCD is the model S of Christensen-Dalsgaard et al. (1996) which also includes diffusion helium and heavy elements, while the Model INV has been constructed using the helium abundance profile as inferred from helioseismic inversions.

profiles inside the Sun are known, it becomes possible to predict the expected neutrino fluxes. Allowing for up to 10% uncertainties in opacities we find that the central temperature of the Sun is in the range  $(15.3\text{-}16.0)\times 10^6$  K and the corresponding neutrino fluxes are between 5.3 - 10.5 SNU for  $^{37}\text{Cl}$  detector, 116-143 SNU for  $^{71}\text{Ga}$  detector and  $(3.7\text{-}8.0)\times 10^6$  cm $^{-2}$ s $^{-1}$  for the  $^8\text{B}$  neutrinos. If larger uncertainties in opacities are permitted, it will be possible to reduce the neutrino fluxes to observed values, but it is not clear if such uncertainties in current estimate of opacities are realistic. Thus, in order to lower the neutrino flux in the  $^{37}\text{Cl}$  experiment to the observed value, the opacities will need to be reduced by a factor of 1.4, for the neutrino flux in the  $^{71}\text{Ga}$  experiment to be decreased to the observed value, opacities will need to be reduced by a factor of 10, while for the  $^8\text{B}$  neutrino flux reduction to the observed value, the opacities need to be cut down by about 15%. But the remarkable feature that emerges is that it becomes impossible to adjust the opacity values to match simultaneously any two of the three solar neutrino experiments. Fig. 2 shows the neutrino fluxes in the three experiments plotted against each other for various seismic models allowing for arbitrary variation in opacity and which produce solar luminosity within 10% of the observed value. Thus each dot in this figure represents a feasible solar model, which is consistent with helioseismic constraints, but there is no restriction on opacities and only mild restriction on luminosity. It can be seen that all feasible models fall in a narrow band and evidently no model which is consistent with helioseismic constraint simultaneously agrees with any two of the three experiments within  $2\sigma$  of the observed values. This clearly suggests that the resolution of the solar neutrino problem should be sought in the realm of non-standard neutrino physics (e.g., MSW effect).

The measured splittings of eigenfrequencies arising from variations in the mode frequencies with different azimuthal order have provided a valuable tool to study the internal rotation rate of the Sun as well as possible departures from spherical symmetry. It may be possible to estimate the solar oblateness from the even order splitting coefficient,  $a_2$ . The current values

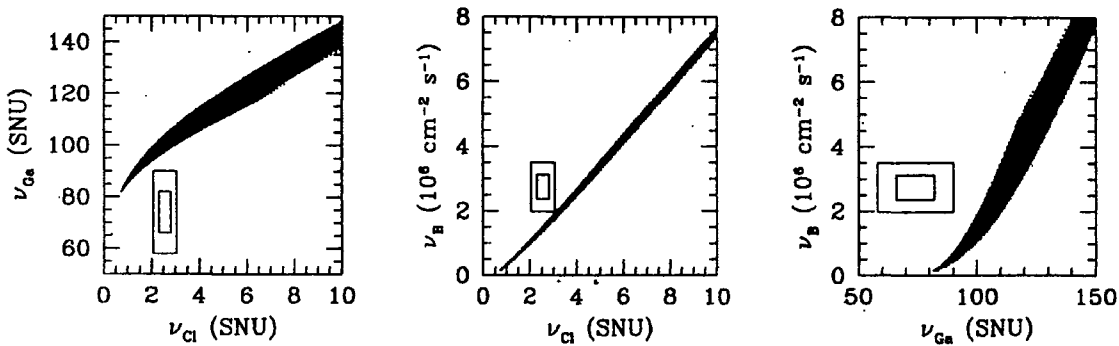


**Figure 2.** Predicted neutrino fluxes for various solar neutrino experiments plotted against each other for possible seismic models allowing for arbitrary variation in opacities. The boxes in each panel represent the  $1\sigma$  and  $2\sigma$  limits on observed fluxes.  $\nu_{ci}$  is the flux for  $^{37}\text{Cl}$  experiment,  $\nu_{\text{Ga}}$  that in  $^{71}\text{Ga}$  experiment and  $\nu_B$  is the  $^8\text{B}$  neutrino flux.

of these coefficients are essentially consistent with zero and provide an upper limit of a few part in  $10^5$  for solar oblateness. With the availability of better data it should be possible to improve the limit on the solar oblateness. Any oblateness of solar body would modify the Sun's gravitational potential and this would induce a precession of the orbit of planet Mercury which provides one of the crucial tests of Einstein's general theory of relativity. The indications from helioseismic data is that less than one percent of the intrinsic precision of Mercury's orbit is likely to arise from the solar oblateness—a result that validates the general theory of relativity.

## References

Antia H.M., Chitre S.M., 1995, *ApJ*, 442, 434.  
 Bahcall J.N., 1989, *Neutrino Astrophysics*, Cambridge University Press, Cambridge, England.  
 Bahcall J.N., Pinsonneault M.H., 1995, *Rev. Mod. Phys.*, 67, 781.  
 Basu S., Antia H.M., 1995, *MNRAS*, 276, 1402.  
 Basu S., Antia H.M., Narasimha D., 1994, *MNRAS*, 267, 209.  
 Christensen-Dalsgaard J., Gough D.O., Thompson M.J., 1991, *ApJ*, 378, 413.  
 Christensen-Dalsgaard J., Däppen W. et al., 1996, *Science*, 272, 1286.  
 Cox A.N., Tabor J.E., 1976, *ApJS*, 31, 271.  
 Cox J.P., Giuli R.T., 1968, *Principles of Stellar Structure*, Gordon and Breach, New York.  
 Gough D.O., Kosovichev A.G., Toomre J. et al., 1996, *Science*, 272, 1296.  
 Guzik J.A., Cox A.N., 1993, *ApJ*, 411, 394.  
 Kosovichev A.G. 1996, *BASI*, 24, 355.  
 Leighton R.B., Noyes R.W., Simon G.W., 1962, *ApJ*, 135, 474.  
 Monteiro M.J.P.F.G., Christensen-Dalsgaard J., Thompson M.J., 1994, *A&A*, 283, 247.  
 Pal P., 1997, *BASI*, (in press).  
 Rogers F.J., Iglesias C.A., 1992, *ApJS*, 79, 507.  
 Roger F.J., Swenson F.J., Iglesias C.A., 1996, *ApJ*, 456, 902.  
 Shibahashi H., Takata M., 1996, *PASJ*, 48, 377.